

# Flavor dependence of jet quenching in heavy-ion collisions from a Bayesian analysis

Shan-Liang Zhang,<sup>1,2,3,\*</sup> Enke Wang,<sup>1,2,†</sup> Hongxi Xing,<sup>1,2,4,‡</sup> and Ben-Wei Zhang<sup>5,§</sup>

<sup>1</sup>*Key Laboratory of Atomic and Subatomic Structure and Quantum Control (MOE),  
Guangdong Basic Research Center of Excellence for Structure and Fundamental Interactions of Matter,  
Institute of Quantum Matter, South China Normal University, Guangzhou 510006, China*

<sup>2</sup>*Guangdong-Hong Kong Joint Laboratory of Quantum Matter,  
Guangdong Provincial Key Laboratory of Nuclear Science, Southern Nuclear Science Computing Center,  
South China Normal University, Guangzhou 510006, China*

<sup>3</sup>*Department of Physics, Hubei University, Wuhan 430062, China*

<sup>4</sup>*Southern Center for Nuclear-Science Theory (SCNT),  
Institute of Modern Physics, Chinese Academy of Sciences, Huizhou 516000, China*

<sup>5</sup>*Institute of Particle Physics and Key Laboratory of Quarks and Lepton Physics (MOE),  
Central China Normal University, Wuhan 430079, China*

(Dated: March 8, 2024)

We investigate the flavor dependence of jet quenching, by performing a systematic analysis of medium modifications on the inclusive jet,  $\gamma$ -jet, and  $b$ -jet in Pb+Pb collisions at the LHC. Our results from MadGraph+PYTHIA exhibit excellent agreement with experimental measurements of the inclusive jet,  $\gamma$ -jet and  $b$ -jet simultaneously in p+p collisions. We then utilize a Bayesian data-driven method to extract systematically the flavor-dependent jet energy loss distributions from experimental data, where the gluon, light quark and  $b$ -quark initiated energy loss distributions are well constrained and satisfy the predicted flavor hierarchy of jet quenching, i.e.  $\langle \Delta E_g \rangle > \langle \Delta E_q \rangle > \langle \Delta E_b \rangle$ . It is shown that the quark-initiated jet energy loss distribution shows weaker centrality and  $p_T$  dependence than the gluon-initiated one. We demonstrate the impacts of the slope of initial spectra, color-charge as well as parton mass dependent jet energy attenuation on the  $\gamma/b$ -jet suppression observed in heavy-ion collisions.

## I. INTRODUCTION

The understanding of strongly interacting nuclear matter at extremely high temperature and energy density is one of the primary subjects in the study of high-energy nuclear collisions at Relativistic Heavy Ion Collider (RHIC)[1, 2] and the Large Hadron Collider (LHC) [3–6]. Jet quenching has long been identified as a very powerful tool to investigate the phase transition from hadron gas to the quark-gluon plasma (QGP) with deconfined quarks and gluons [7, 8], and numerous studies have shown that parton energy loss in the QGP may lead to the suppression of the single inclusive hadron/jet spectra [9–15], the shift of  $\gamma/Z$ +hadron/jet correlations [16–31] and dihadron transverse momentum asymmetry [32–35], the modification of jet internal structures [36–44], as well as the azimuthal anisotropy ( $v_2$ ) of hadrons and jets [45–48] with the large transverse momentum ( $p_T$ ) in nucleus-nucleus (A+A) collisions, by comparison with those in proton-proton (p+p) collisions [49–51].

The interaction between an energetic parton and the QGP is sensitive to the colour charge and the mass of the parton, while medium-induced gluon radiation is expected to be enhanced for gluon due to its larger color factor, and to be suppressed for heavy quarks by the

dead-cone effect relative to that for light quarks [52–55]. Such a predicted flavor hierarchy of jet quenching can be identified by a separate determination of quark and gluon jet energy loss, which could play a significant role in revealing the fundamental color structures of the QGP and testing the color representation dependence of the jet-medium interaction [56, 57]. This however proves difficult, as the final state hadronic observables are a mixture of quark and gluon contributions. A clean method for identifying quark or gluon energy loss remains a challenge, despite many past attempts such as the multivariate analysis of jet substructure observables [58], the proposal of using the averaged jet charge [59–61] and electroweak gauge boson tagged jet [23–28, 30, 62–64].

One recent important measurement by the ATLAS Collaboration, i.e. the nuclear modification factor for  $\gamma$ -tagged and  $b$ -tagged jets [65, 66], shows quite different modification pattern from that of single inclusive jets [67]. It is reported that the  $\gamma$ -tagged jets  $R_{AA}$  [65] are much higher and show a weaker centrality dependence than inclusive jet  $R_{AA}$  [67], indicating a sensitive observation of color factor dependence of jet-medium interaction. In addition, the ratio of  $R_{AA}$  between  $\gamma$ -tagged jet and inclusive jets are above most of the theoretical model calculations [65], which challenges the implemented color charge dependence of energy loss in these models. Likewise, systematic difference between  $b$ -jets and inclusive jets  $R_{AA}$  are also observed [66] and, suggesting a role for mass and colour charge effects in partonic energy loss in heavy-ion collisions. Those differences may arise from not only the inclusive jet mixture of quarks and gluons, where gluon lose more energy, but

\* Corresponding author.  
zhangshanl@m.scnu.edu.cn

† wangke@scnu.edu.cn

‡ Corresponding author.

hxxing@m.scnu.edu.cn

§ bwzhang@mail.ccnu.edu.cn

also the slope of their initial spectrum [68]. Meanwhile, most theoretical models can capture the inclusive jet  $R_{AA}$  [67]. However, discrepancies arise when examining the latest photon/ $b$ -tagged jet  $R_{AA}$  data points and the double ratio  $R_{AA}^{\gamma/b+\text{jet}}/R_{AA}^{\text{inclusive jet}}$  [65, 66]. In general, these quantities tend to surpass the predictions of many jet quenching models grounded in pQCD calculations and kinetic theory. Such contradictions strongly motivate a data-driven Bayesian analysis to extract the model-independent yet flavor-dependent jet energy loss distributions, which can not only identify the transport properties of QGP [69], but also help to pin down the uncertainties of jet quenching models.

The purpose of this work is to extract the flavor-dependent and model-independent jet energy loss distributions by performing a systematic study of the medium suppression of the inclusive jet,  $\gamma$ +jet, and  $b$ -jet in Pb+Pb collisions relative to that in p+p in a unified framework simultaneously. In the numerical calculation of the p+p baseline, a Monte Carlo event generator MadGraph5+PYTHIA8 [70], which can perform the next-to-leading order (NLO) matrix element (ME) matched to the resummation of parton shower (PS) calculations, is employed to simulate initial hard partons with shower partons and jet cross sections in p+p collisions. Specifically, a Bayesian data-driven analysis [71] of the nuclear modification factors of inclusive jet [67],  $\gamma$ +jet [65], and  $b$ -jet [66] is performed to quantitatively extract the flavor dependent jet energy loss distributions, which satisfies the predicted flavor hierarchy of jet quenching. We study the relative contributions from the slope of initial spectra, color-charge as well as parton mass dependent jet energy attenuation to the  $\gamma/b$ -jet suppression in heavy-ion collisions at the same time.

The remainder of the paper is organized as follows. In Sec. II we first introduce the framework. With a systematic study of the inclusive jet,  $\gamma$ +jet, and  $b$ -jet productions in p+p collisions using MadGraph+Pythia, a Bayesian data-driven analysis of nuclear modification factors of these processes is performed to quantitatively extract flavor dependent jet energy loss distributions in Sec. III. Finally, a summary is presented in Sec. IV.

## II. FRAMEWORK

In order to study the flavor dependence of jet energy loss, we express the final observable of the nuclear modification factor  $R_{AA}$  in a given centrality in terms of the flavor dependent  $R_{AA}^{i,C}$ ,

$$R_{AA}^C = \frac{\sum_i R_{AA}^{i,C} d\sigma_{pp}^i}{\sum_i d\sigma_{pp}^i} = R_{AA}^{g,C} + \sum_{i \neq g} (R_{AA}^{i,C} - R_{AA}^{g,C}) f_i, \quad (1)$$

where the superscripts  $i$  and  $C$  stand for the parton flavor and centrality, respectively.  $d\sigma_{pp}^i$  is the differential cross section for parton  $i$  initiated jet in p+p collisions,  $f_i =$

$d\sigma_{pp}^i / \sum_i d\sigma_{pp}^i$  is the fraction of the total jet cross section from the parton  $i$  initiated one.

In our analysis, the flavor and centrality dependent nuclear modification factor  $R_{AA}^{i,C}$  is assumed to be factorized as the convolution of its cross section in p+p collisions and the corresponding parton energy loss distribution [68, 71]

$$R_{AA}^{i,C}(p_T) = \frac{\int d\Delta p_T d\sigma_{pp}^i(p_T + \Delta p_T) \otimes W_{AA}^{i,C}(x)}{d\sigma_{pp}^i(p_T)}, \quad (2)$$

where  $x = \Delta p_T / \langle \Delta p_T \rangle$  is the scaled variable with  $\Delta p_T$  the amount of energy loss and  $\langle \Delta p_T \rangle$  the averaged jet energy loss, which can be parametrized as  $\langle \Delta p_T \rangle = \beta_i(p_T)^{\gamma_i} \log(p_T)$  following Refs. [36, 68]. In Eq. (2),  $W_{AA}^{i,C}$  is the scaled energy loss distribution of parton  $i$  in a given centrality class  $C$  of A+A collisions and can be assumed as:

$$W_{AA}^i(x) = \frac{\alpha_i^{\alpha_i} x^{\alpha_i-1} e^{-\alpha_i x}}{\Gamma(\alpha_i)} \quad (3)$$

where  $\Gamma$  is the standard Gamma-function, and the above functional form can be empirically interpreted as the energy loss distribution resulting from  $\alpha_i$  number of jet-medium scattering in the medium.

In this setup, for each parton flavor  $i$ , the scaled jet energy loss distributions  $W_{AA}^i(x)$  can be determined by three parameters,  $\alpha_i, \beta_i, \gamma_i$ . According to this flavor decomposition, one can extract  $\alpha_i, \beta_i, \gamma_i$ , for each parton flavor  $i$  to determine the flavor and centrality dependent jet energy loss distributions  $W_{AA}^i(x)$  through a global analysis by combining the simulations of p+p cross section and the measurements of nuclear modification factor  $R_{AA}$  for jet related observables.

We apply an advanced statistical tool, i.e. Bayesian analysis, for this purpose. Such a method has been successfully employed to extract the bulk and heavy quark [72], jet [71] and gluon [69] energy loss distributions as well as jet transport coefficients [73, 74] in heavy-ion collisions. The process can be summarized as

$$P(\theta|data) = \frac{P(\theta)P(data|\theta)}{P(data)}, \quad (4)$$

where  $P(\theta|data)$  is the posterior distribution of parameters  $\theta$  given the experimental data,  $P(\theta)$  is the prior distribution of  $\theta$ ,  $P(data|\theta)$  is the Gaussian likelihood between experimental data and the output for any given set of parameters and  $P(data)$  is the evidence. Uncorrelated uncertainties in experimental data are used in the evaluation of the Gaussian likelihood. To estimate the posterior distribution given by Eq. 4, the Markov chain Monte Carlo (MCMC) process is carried out using the Metropolis-Hasting algorithm [75]. A uniform prior distribution  $P(\theta)$  in the region  $[\alpha_i, \beta_i, \gamma_i] \in [(0, 10), (0, 8), (0, 0.8)]$  is used for the Bayesian analysis. We first run  $2 \times 10^6$  burn-in MCMC steps to allow the chain to reach equilibrium, and then generate  $2 \times 10^6$  MCMC steps in parameter space.

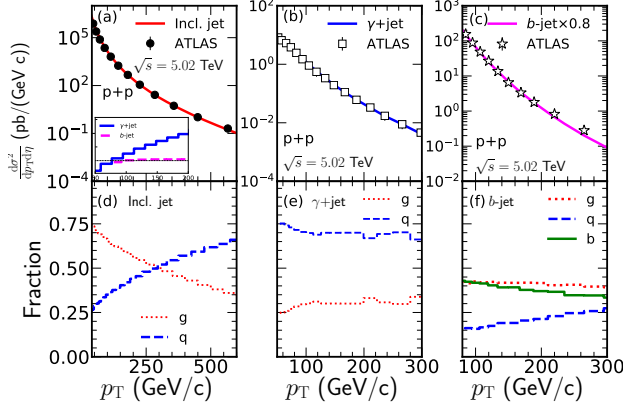


FIG. 1. (Color online) Up: Transverse momentum distributions of: (a) inclusive jet, (b)  $\gamma$ -tagged jet, and (c)  $b$ -jet simulated by MadGraph+Pythia8 (lines) and the comparison with experimental data (samples) [65–67] in p+p collisions. The inset in (a) is the ratio of  $\gamma$ -tagged jet (blue solid) and  $b$ -jet (red dashed) to inclusive jet cross section. Bottom: fraction of quark (Dashed blue line) and gluon (Solid red line) initiated jet of : (d) inclusive jet, (e)  $\gamma$ -tagged jet, and (f)  $b$ -jet as a function of jet  $p_T$  in p+p collisions.

### III. RESULTS AND DISCUSSIONS

#### A. Cross sections in p+p

In our analysis, we consider three different observables, i.e. the inclusive jet,  $\gamma$ -jet and  $b$ -jet, to study the flavor dependence of jet energy loss distribution. Considering the facts NLO matching have considerable contributions to  $b$ -jet cross section [76] and  $\gamma$ -jet [27], we simulate  $d\sigma_{pp}^i$  using a Monte Carlo event generator MadGraph5+PYTHIA8 [70], which combines the NLO matrix element (ME) with the matched parton shower (PS). Furthermore, those shower partons are reconstructed using the anti- $k_T$  algorithm [77] implemented in the FastJet [78]. In order to compare with the  $b$ -jet measurements, we define  $b$ -jet to be the one that contains at least one  $b$ -quark (or  $\bar{b}$ -quark) with momentum  $p_T > 5$  GeV/c and a radial separation from the reconstructed jet axis  $\Delta R < 0.3$ . In ATLAS measurements [65–67], inclusive jet and  $\gamma$ -jet are reconstructed with  $R = 0.4$  and accepted in the rapidity range of  $|y| < 2.8$ , while  $b$ -jet are reconstructed with  $R = 0.2$  and accepted within  $|y| < 2.1$ . Besides, for  $\gamma$ -jet event,  $\gamma$  is required to have  $p_T^\gamma > 50$  GeV/c, and a cut  $\Delta\phi_{j\gamma} > \pi/2$  is imposed to select the back-to-back  $\gamma$ -jet pairs. In our simulations, we implement correspondingly the same kinematic cuts adopted by experiments.

In the top panel of Fig. 1, we plot the differential cross section of: (a) inclusive jet (denoted as “Incl. jet” in the figure in the following), (b)  $\gamma$ -jet, and (c)  $b$ -jet as a function of jet transverse momentum  $p_T$  obtained from MadGraph+Pythia8 simulation at 5.02 TeV in p+p collisions. Through the comparison with experimental data [65–67],

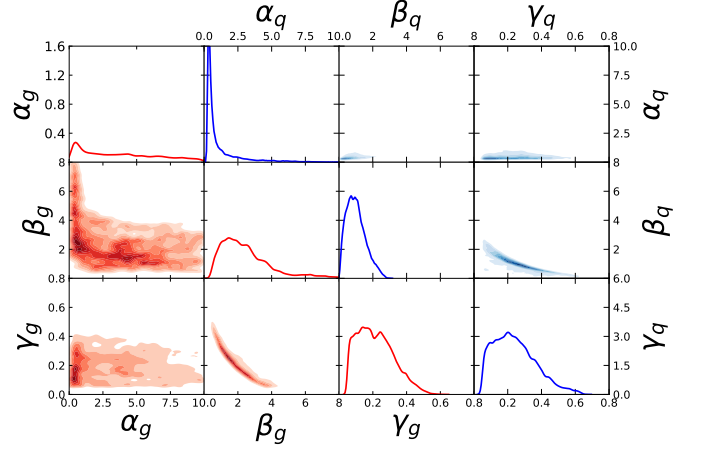


FIG. 2. (Color online) Distributions of and the correlations between the Bayesian-extracted parameters for gluon (left) and quark (right) initiated jet energy loss via fitting to  $R_{AA}$  of inclusive jet and  $\gamma$ -tagged jet in central 0-10% Pb+Pb collisions at 5.02 TeV [65, 67].

one can see clearly that the simulations give very well descriptions of all experimental data. Notice that the inset of Fig. 1(a) is the scaled ratio of  $\gamma$ -jet (blue solid) and  $b$ -jet (red dashed) cross section to that of inclusive jet. In Fig. 1(a-c), one can see that the inclusive jet spectrum is much steeper than  $\gamma$ -jet, while  $b$ -jet have similar slope as the inclusive jet, consistent with the results of Refs. [65, 66].

In order to study the flavor dependence of jet energy attenuation in heavy ion collisions, we present the relevant contributions in terms of jet flavor, which is defined as the flavor of the hard parton that fragments into the final observed jet<sup>1</sup>. In the bottom panel of Fig. 1, we show the fraction from quark- and gluon- initiated jet in: (d) inclusive jet, (e)  $\gamma$ -jet, and (f)  $b$ -jet as a function of jet  $p_T$ . One can see that for inclusive jet, the contribution from gluon (quark) initiated jet dominates in low (large)  $p_T$  region, and gradually decreases (increases) with increasing  $p_T$ . While for  $\gamma$ -jet, the quark initiated jet dominates ( $\sim 80\%$ ) in the whole  $p_T$  region. For  $b$ -jet, it can be generated either from the initial hard scattering or from the parton showers via gluon and quark splitting. In the first case, it is the  $b$ -quark that initiates the  $b$ -jet, the relevant contribution is shown by  $b$ -quark in Fig. 1(f). In heavy-ion collisions, the medium modification to such  $b$ -jet has direct connection to the heavy quark energy loss [53–55, 79]. On the other hand, the medium modification on the latter two cases (with gluon and quark splitting) would resemble that of a massive quark or gluon jets. As can be seen,  $b$ -jet from gluon initiated contributes about 40% to the cross section in the whole  $p_T$  region, while the light quark initiated con-

<sup>1</sup> If  $\geq 2$  hard partons locate in the final observed jet, the flavor of a jet is defined as that of the hardest parton.

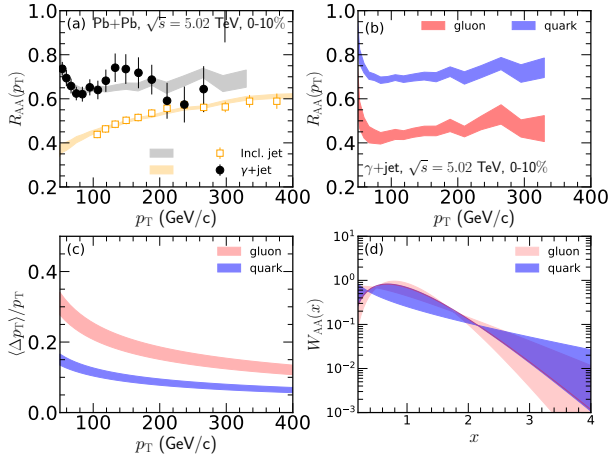


FIG. 3. (Color online) (a) Data-driven Bayesian fitted nuclear modification factor  $R_{AA}$  of inclusive jet (orange) and  $\gamma$ -tagged jet (gray) and the comparison to experimental data at [65, 67]. (b) Data-driven extracted nuclear modification factor of quark (blue) and gluon (red) initiated  $\gamma$ +jet. (c) Fraction of jet average energy loss of light quark (blue) and gluon (red) initiated jet, (d) scaled energy loss distributions  $W_{AA}^i(x)$  of quark (blue) and gluon (red) initiated jet.

tribution goes up with increasing  $p_T$ .

### B. Colour-charge dependence of $R_{AA}$

In Fig. 2, we present the distributions of the final-extracted parameters for gluon (left) and quark (right) initiated jet energy loss as well as their correlations, via Bayesian-fitting to the ATLAS data [65, 67] on  $R_{AA}$  of inclusive jets and  $\gamma$ -tagged jets in 0-10% Pb+Pb collisions at 5.02 TeV simultaneously. As can be seen,  $\beta_i$  and  $\gamma_i$ , which reflect the average energy loss, are strongly correlated and well constrained for quark and gluon initiated jet. The mean value as well as its standard deviation of those final extracted parameters for gluon and charm quark energy loss distribution are summarized in Table I.

The final fitted nuclear modification factor  $R_{AA}$  of inclusive jet and  $\gamma$ -tagged jet as well as the comparison to experimental data [65, 67] in 0-10% centrality at 5.02 TeV are shown in Fig. 3.(a), and data-driven extracted nuclear modification factor of quark- and gluon- initiated  $\gamma$ +jet are shown in Fig. 3.(b). The corresponding bands are results with one sigma deviation from the average fits of  $R_{AA}$ . Considering the fact that the training process will minimize the Gaussian likelihood function between experimental data and the output for any given set of parameters, the final fitted results are almost close to the central value of data points. Moreover, considering the limited experimental data sets, our parametrization for the energy loss distribution shown in Eq. (3) is limited to three parameters for each flavor, which could introduce correlations between different data bins. Therefore, the MCMC bands is more restricted than the uncertainty in the experimental data. We leave a more detailed anal-

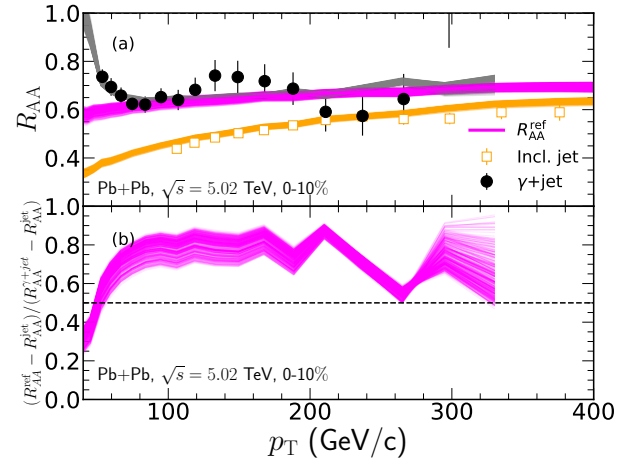


FIG. 4. (Color online) (a) The reference  $R_{AA}^{\text{ref}}$  (magenta) and the comparison with  $R_{AA}$  of  $\gamma$ +jet (grey) and inclusive jet (orange) jet in 0-10% centrality at 5.02 TeV, and the comparison with experimental data [65]. (b) The relative contribution fraction from large quark fraction to the less suppression of  $\gamma$ +jet  $R_{AA}$  compared to inclusive jet  $R_{AA}$ .

ysis of the uncertainties for a future publication. Data-driven extracted average energy loss fraction  $\langle \Delta p_T \rangle / p_T$  and scaled energy loss distributions  $W_{AA}(x)$  of quark and gluon initiated jet are also presented in Fig. 3.(c) and Fig. 3.(d). As can be seen, average energy loss of gluon and quark jet is well constrained in  $p_T < 200$  GeV/c, but is weaker constrained at high  $p_T$  due to large experimental data errors and the scarcity of  $\gamma$ -tagged jet experimental data at such high  $p_T$ . The quark-initiated jets lose less fraction of its energy and shows a weaker dependence on the jet  $p_T$  compared to gluon-initiated jets due to its color factor as expected. Since jet showers also contain gluons even if they are initiated by a hard quark, the net energy loss of a gluon-tagged jet is always larger than that of a quark-tagged jet but the ratio is smaller than 9/4 from the naive leading order estimation [80–82].

Fig. 3.(a) shows that  $\gamma$ -tagged jet  $R_{AA}$  is less suppressed compared to that for inclusive jet, which is a mix effect of the slope of initial spectra and parton color-charge in p+p collisions. To clarify the relative contributions from the color-charge effect and the initial parton spectra between  $\gamma$ -tagged jet and inclusive jet, we calculate an artificial reference  $R_{AA}^{\text{ref}}$  following Eq.(1), by assuming the inclusive jet production has the same fraction of quark jet as  $\gamma$ +jet. This reference  $R_{AA}^{\text{ref}}$  is shown by magenta lines in Fig. 4.(a). The difference between  $R_{AA}^{\text{ref}}$  and inclusive jet  $R_{AA}$  (denoted as “ $R_{AA}^{\text{jet}}$ ”) should be attributed largely to the different color-charge effect between quark-medium and gluon-medium interactions, while the distinction between  $R_{AA}^{\text{ref}}$  and  $\gamma$ +jet  $R_{AA}$  (denoted as “ $R_{AA}^{\gamma+\text{jet}}$ ”) should be attributed mostly to the slope of reference spectra in p+p.

Fig. 4.(b) shows the relative contribution fraction from large quark fraction, evaluated as  $f^{\text{flavor}} = (R_{AA}^{\text{ref}} - R_{AA}^{\text{jet}}) / (R_{AA}^{\gamma+\text{jet}} - R_{AA}^{\text{jet}})$ , to the less suppression of  $\gamma$ +jet

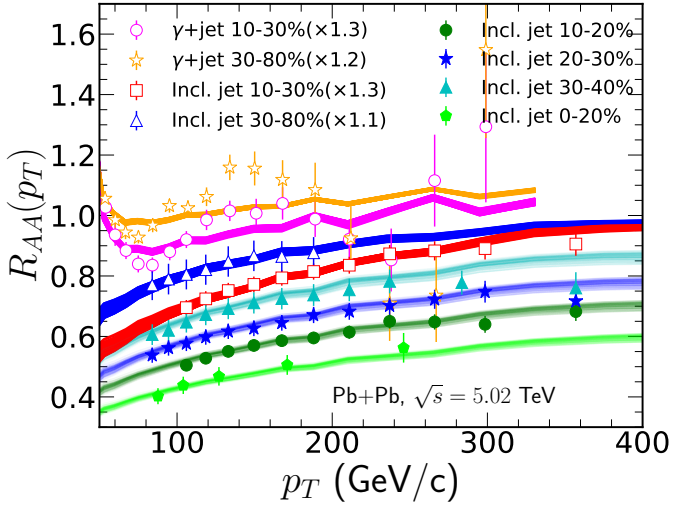


FIG. 5. (Color online) Data-driven fitted nuclear modification factor  $R_{AA}$  of the inclusive jet  $R_{AA}$  [67] and  $\gamma$ +jet  $R_{AA}$  [65] in 10-30%, 30-80% centrality bins and predictions of inclusive jet  $R_{AA}$  in 10-20%, 20-30%, 30-40% and 0-20% centrality bins as well as the comparison with experimental data [67].

TABLE I. Parameters  $[\alpha_i, \gamma_i, \beta_i]$  of quark and gluon jet energy loss distribution from Bayesian fits to experimental data [65, 67] on inclusive jet and  $\gamma$ +jet suppressions at 5.02 TeV.

		$\alpha_i$	$\beta_i$	$\gamma_i$
0-10%	gluon	$4.36 \pm 2.07$	$1.78 \pm 0.38$	$0.25 \pm 0.03$
	quark	$0.5 \pm 0.07$	$0.39 \pm 0.17$	$0.32 \pm 0.13$
10-30%	gluon	$2.17 \pm 0.94$	$1.47 \pm 0.44$	$0.25 \pm 0.04$
	quark	$5.81 \pm 1.8$	$1.27 \pm 0.12$	$0.09 \pm 0.02$
30-80%	gluon	$4.78 \pm 1.87$	$1.16 \pm 0.17$	$0.11 \pm 0.03$
	quark	$6.4 \pm 2.63$	$0.7 \pm 0.05$	$0.09 \pm 0.01$

$R_{AA}$  compared to inclusive jet  $R_{AA}$ . The increased quark jet fraction in inclusive jet production give the dominant contributions to the difference of  $R_{AA}$  between  $\gamma$ +jet and inclusive jet at  $p_T > 60$  GeV/c. Then  $1 - f^{\text{flavor}}$  characterized approximately the relative contribution from the slope of reference spectra, which plays a dominated role in the suppression at low  $p_T$ . Besides, the distinction between  $\gamma$ +jet  $R_{AA}$  and inclusive jet  $R_{AA}$  will diminish with increasing  $p_T$ , because quark-initiated jets contribute a lion's share to the yields of both  $\gamma$ +jet and the inclusive jet at very large  $p_T$ , which can be verified with the upcoming high precision measurements at the LHC.

### C. Centrality dependence of $R_{AA}$

Moreover, we extract the centrality dependent quark and gluon jet energy loss distributions before exploring parton-mass effect on jet quenching motivated by two reasons. First,  $\gamma$ -tagged jet  $R_{AA}$  [65] shows a weaker dependence on centrality compared to inclusive jet [67],

indicating that gluon-initiated jets may show a distinct centrality dependence with quark-initiated jets. Second, the experimental data of  $\gamma$ +jet  $R_{AA}$  [65], inclusive jet  $R_{AA}$  [67] and  $b$ -jet  $R_{AA}$  [66] are in different centrality bins. We need centrality dependent quark and gluon jet energy loss distributions to fit  $\gamma$ +jet  $R_{AA}$ , inclusive jet  $R_{AA}$  and  $b$ -jet  $R_{AA}$  simultaneously.

As a matter of fact, there are no experimental data of inclusive jet  $R_{AA}$  and  $\gamma$ +jet  $R_{AA}$  in the same centrality class except in central 0-10% centrality. For inclusive jet measurements, the existing measurements are provided for centrality bins 0-10%, 10-20%, 20-30%, 30-40%, 40-50%, 50-60%, 60-70%, 70-80% [67], while for  $\gamma$ +jet  $R_{AA}$ , it is limited to 0-10%, 10-30%, 30-80% [65]. In order to take full advantage of the existing measurements for inclusive jet  $R_{AA}$  in different centrality bins, we generate the inclusive jet  $R_{AA}$  as well as the corresponding errors in 10-30% and 30-80% centrality bins according to  $R_{AA}^C = \sum_{c \in C} P^c R_{AA}^c$ , where  $P^c = N_{\text{bin}}^c / \sum_c N_{\text{bin}}^c$  is the probability of finding jet events in a given centrality bin following Ref. [83]. With such an extension, we can perform a simultaneous fit for both inclusive jet  $R_{AA}$  and  $\gamma$ +jet  $R_{AA}$  in 10-30% and 30-80% centralities. In Fig. 5, we present the data-driven fitted nuclear modification factor  $R_{AA}$  of inclusive jet [67] and  $\gamma$ +jet [65] in 10-30% and 30-80% centralities and the comparison with experimental data at 5.02 TeV. All final spectra based on Eq. (1) and Eq. (2) are in nice agreement with the experimental data. The corresponding mean value as well as its standard deviation of those final extracted parameters for gluon and light quark energy loss distribution are summarized in Table I.

Meanwhile, we obtain  $R_{AA}$  for quark-initiated jets and gluon-initiated jets in 10-30%, 30-80% centrality. Combined with the flavor dependent  $R_{AA}$  in 0-10% as extracted in the previous section (Fig. 3.(b)), we obtain the centrality dependence of final fitted gluon-initiated jet, quark-initiated jet and inclusive jet  $R_{AA}$ . In Fig. 6, we show the centrality dependence of final fitted gluon jet (red), quark jet (blue) and inclusive jet (green)  $R_{AA}$  in Pb+Pb collisions in the region  $100 < p_T < 112$  GeV/c by step lines. One finds that the quark-initiated jet has weaker dependence on the centrality than that for gluon-initiated jet.

Next, we can fit the centrality dependent  $R_{AA}$  of quark- and gluon- initiated jet via a simple parametrization  $h^i(C) = a_i C^2 + b_i C + c_i$ , with  $C$  stands for the centrality. The best fit curves of  $h^i(C)$  are shown in Fig. 6 by blue and red band, and the corresponding best-fit parameter values are presented in Table. II. Notice that the extrapolation to peripheral collisions ( $> 80\%$ ) is greater than one and can not be trusted, a reasonable identification of jet energy loss distribution for peripheral collisions would require a corresponding extension of experimental measurements. If we ignore the  $p_T$  dependence of  $h^i(C)$ ,  $R_{AA}^{i,C}$  for any centrality  $C$  can be simply obtained by  $R_{AA}^{i,C} = h^i(C) * R_{AA}^{i,rc} / h^i(rc)$ , where  $rc$  stands for reference centrality. Based on Eq. (1) and the above extracted centrality dependent quark and gluon jet  $h^i(C)$ , the pred-

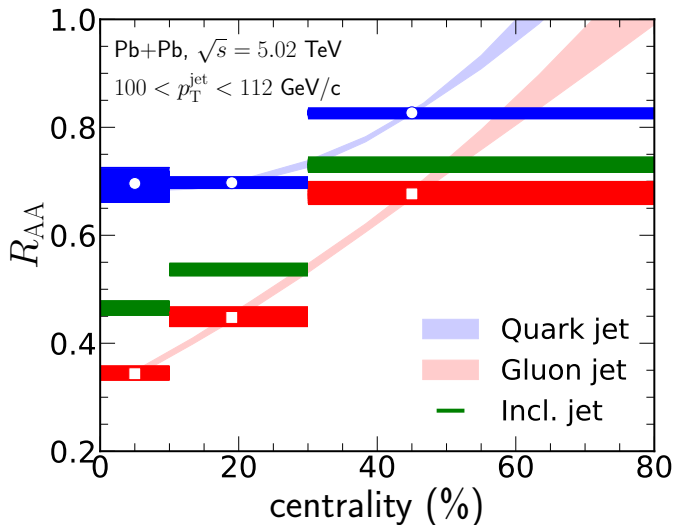


FIG. 6. (Color online) The centrality dependence of final fitted gluon jet (red), quark jet (blue) and inclusive jet (green)  $R_{AA}$  in Pb+Pb collisions at 5.02 TeV.

TABLE II. The best-fitted Parameters  $[a_i, b_i, c_i]$  for centrality dependent quark and gluon jet energy loss distributions.

	$a_i (\times 10^{-5})$	$b_i (\times 10^{-3})$	$c_i$
Quark	$12.39 \pm 2.83$	$-2.95 \pm 1.74$	$0.7 \pm 0.021$
Gluon	$3.36 \pm 2.45$	$6.65 \pm 1.20$	$0.309 \pm 0.00879$

TABLE III. Parameters  $[\alpha_i, \gamma_i, \beta_i]$  for gluon, quark and  $b$ -quark energy loss in 0-20% centrality from fitting to  $\gamma$ -jet  $R_{AA}$  [65], inclusive jet  $R_{AA}$  [67] and  $b$ -jet  $R_{AA}$  [66] at  $\sqrt{s} = 5.02$  TeV simultaneously.

(0-20%) 5.02 TeV			
	$\alpha_i$	$\beta_i$	$\gamma_i$
Gluon	$4.60 \pm 2.96$	$2.18 \pm 1.12$	$0.21 \pm 0.12$
Quark	$4.12 \pm 2.71$	$0.86 \pm 0.38$	$0.24 \pm 0.11$
$b$ -quark	$5.32 \pm 2.84$	$0.80 \pm 0.54$	$0.2 \pm 0.17$

ication of inclusive jet  $R_{AA}$  in 0-20%, 10-20%, 20-30%, 30-40% are presented in Fig. 5. One can see that our extracted centrality dependence of quark and gluon jet energy loss distributions can describe the experimental data  $R_{AA}$  [67] very well.

#### D. Parton-mass dependence of $R_{AA}$

Finally, with the extracted centrality dependent quark and gluon energy loss distributions, we also extract  $b$ -jet energy loss in the same framework based on Eqs. (1) and (2) through fitting to the experimental data of  $b$ -jet  $R_{AA}$  [66], inclusive jet  $R_{AA}$  in 0-20% centrality [67] and  $\gamma$ -tagged jet  $R_{AA}$  in 0-10% [65] simultaneously. Considering the recent CMS measurements [50, 84], as well as an earlier ATLAS measurement [85], where the ratio of

inclusive jet  $R_{AA}$  with jet cone  $R=0.4$  to  $R=0.2$  show no deviation from one at large  $p_T$ , and the limited  $b$ -jet data points, we ignore the jet cone dependence at present and mainly focus on a qualitative investigation on the parton mass/ flavor effects on the  $b$ -jet  $R_{AA}$ .

The final fitted nuclear modification factor  $R_{AA}$  of  $b$ -jet (lime green band), inclusive jet (magenta band) and  $\gamma$ -tagged jet (gray band) as well as the comparison with experimental data [65–67] are shown in Fig. 7(a). The corresponding bands are results with one sigma deviation from the average fits of  $R_{AA}$ . Meanwhile, Fig. 7(b) shows the extracted nuclear modification factor  $R_{AA}$  for  $b$ -quark initiated (green, denoted as “ $R_{AA}^b$ ”), light-quark (denoted as “ $R_{AA}^{\text{quark}}$ ”) and gluon (denoted as “ $R_{AA}^{\text{gluon}}$ ”) initiated  $b$ -jet in 0-20% centrality, with the corresponding parameters for gluon, quark and  $b$ -quark energy loss distribution summarized in Table.III. The final extracted light-quark and gluon initiated jet energy loss distributions are consistent with our previous results in the same centrality, while  $b$ -quark initiated jets is less suppressed compared to light-quark initiated jets due to its large mass in low  $p_T$  region. Our result shows a clear flavor hierarchy of jet energy loss at high energies,  $\langle \Delta E_g \rangle > \langle \Delta E_q \rangle > \langle \Delta E_b \rangle$  inside a hot nuclear matter, consistent with perturbative QCD expectation.

To explore the underlying  $b$ -jet suppression mechanism in heavy-ion collisions, we also present in Fig. 7(c) the ratio of  $b$ -quark initiated jets  $R_{AA}$  to light quark initiated jet  $R_{AA}$  as  $R_{AA}^b / R_{AA}^{\text{quark}}$ , and also in Fig. 7(d) the ratio of  $b$ -jet  $R_{AA}$  (denoted as “ $R_{AA}^{b\text{-jet}}$ ”) to inclusive jet  $R_{AA}$   $R_{AA}^{b\text{-jet}} / R_{AA}^{\text{jet}}$  extracted from global analysis and the comparison to the experimental measurements [66]. Our numerical results can describe the experimental data within large uncertainties [66]. Those ratios are greater than unity and go down with increasing  $p_T$ , indicating that the parton mass effect is reduced with increasing  $p_T$  [86]. However, the mass effect for  $b$ -jet could persist to large  $p_T$ , even at  $p_T \sim 300$  GeV/c, and is consistent with the current data and a model based on strong coupling (via the AdS/CFT correspondence) [87], in contrast to Ref. [83, 86] in which mass effects are expected to be small at  $p_T > 70$  GeV/c. Those disagreements may be explained by two reasons. For one thing, due to the subdominant contributions and the limited  $b$ -jet  $R_{AA}$  data points with large uncertainties, especially at large  $p_T$ , which have weak constraints on  $b$ -quark initiated jet,  $b$ -quark initiated jet energy loss distributions is weakly constrained at present. For another, this may be attributed to the mixture of mass effect and color effect, as we may show below.

Notice that  $b$ -jet spectra [66] have similar slope as the inclusive jet as shown in the inset of Fig. 1(a), so the parton mass and color effects may give the dominated contributions to the difference between inclusive jet  $R_{AA}$  and  $b$ -jet  $R_{AA}$ . For further demonstration of  $b$ -quark mass effect on the suppression of  $b$ -jet, we show in Fig. 7(d) (yellow band) the ratio of  $b$ -jet  $R_{AA}$  to inclusive jet  $R_{AA}$ , assuming  $b$ -jet has the same fraction of gluon

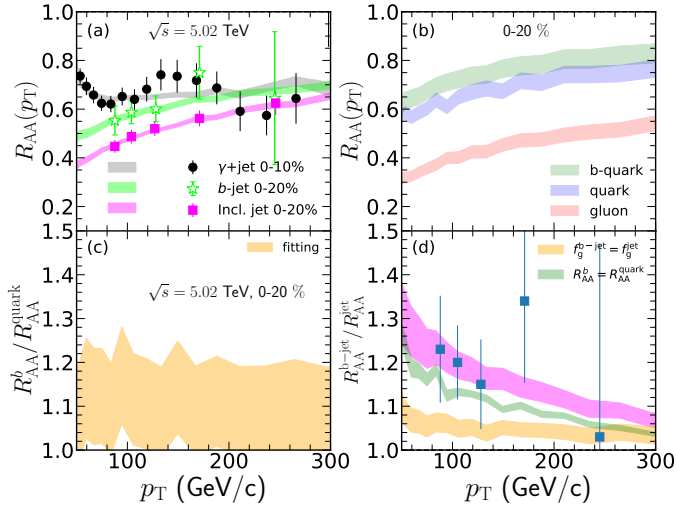


FIG. 7. (Color online) (a): final fitted nuclear modification factor  $R_{AA}$  of  $b$ -jets (lime green), inclusive jet (magenta) and  $\gamma$ -tagged jet (gray) and the comparison with experimental data [65–67]. (b): the data-driven extracted  $R_{AA}$  of gluon (red), light quark (blue), and  $b$ -quark (green) initiated jets. (c): The ratio of  $R_{AA}^b / R_{AA}^{\text{quark}}$  from global analysis. (d): the ratio of  $R_{AA}^{b\text{-jet}} / R_{AA}^{\text{jet}}$  extracted from global analysis and the comparison to the experimental measurements. The quark mass effect (yellow) and less gluon fraction effect (green) to the ratio of  $R_{AA}$  are also presented.

initiated jet as inclusive jet (denoted as “ $f^{b\text{-jet}} = f^{\text{jet}}$ ”). The difference between this ratio and  $R_{AA}^{b\text{-jet}} / R_{AA}^{\text{jet}}$  should be attributed to the  $b$ -quark mass effect. One can see that the deviation between  $b$ -jet and the inclusive jet is moderately reduced with increasing  $p_T$ . The mass effect roughly give considerable contributions to the ratio of  $R_{AA}^{b\text{-jet}} / R_{AA}^{\text{jet}}$  and are expected to be small at  $p_T \sim 300$  GeV/ $c$ .

To further illustrate the color-charge effect on the suppression of  $b$ -jet, we also calculated the ratio of  $b$ -jet  $R_{AA}$  to inclusive jet  $R_{AA}$ , assuming  $b$ -quark jet lose the same fraction of energy as light-quark initiated jet (denoted as “ $R_{AA}^b = R_{AA}^{\text{quark}}$ ”), as shown by green band in Fig. 7(d). The difference between this ratio and  $R_{AA}^{b\text{-jet}} / R_{AA}^{\text{jet}}$  should be attributed to the different gluon and quark fraction. As can be seen, those ratio is significantly enhanced and also show a downward tendency with increasing  $p_T$ , indicating that, less gluon initiated jet contribution also lead to the less suppression of  $b$ -jet compared to inclusive jet in heavy-ion collisions, especially in low  $p_T$  region. Therefore, we can see that the color charge effect have greater impacts to the ratio  $R_{AA}^{b\text{-jet}} / R_{AA}^{\text{jet}}$  than parton mass effect in heavy-ion collisions. Furthermore, the contribution from gluon initiated jet to inclusive jet production is greater than that to  $b$ -jet in the  $p_T < 300$  GeV/ $c$  region as shown in Fig. 1. Thus  $b$ -jet  $R_{AA}$  is moderately larger than inclusive jet  $R_{AA}$ .

## IV. SUMMARY

We have carried out a systematic investigation of parton color-charge and parton mass dependence of nuclear modification factor by a systematic study of the medium modifications on three full jet observables: the inclusive jet,  $\gamma$ +jet, and  $b$ -jet, in Pb+Pb collisions relative to that in p+p at the LHC. Our results from MadGraph+PYTHIA give very nice descriptions of the experimental data for these three jet observables in p+p. Then a Bayesian data-driven method is applied to extract the model-independent but flavor-dependent jet energy loss distributions. Fitting to those experimental data simultaneously, we present the first quantitative extraction of gluon, light quark and  $b$ -quark initiated jet energy loss distributions in heavy-ion collisions. It is seen that the energy loss of quark-initiated jets shows a weaker centrality dependence and weaker  $p_T$  dependence compared to that of gluon-initiated jets. Our result shows a clear flavor hierarchy of jet energy loss at high energies,  $\langle \Delta E_g \rangle > \langle \Delta E_q \rangle > \langle \Delta E_b \rangle$  inside a hot nuclear matter, consistent with perturbative QCD expectation.

Furthermore, we analysed the relative contributions from the slope of initial spectra, parton color-charge as well as parton mass dependent jet energy attenuation to the  $\gamma$ /b-jet suppression in heavy-ion collisions. We find that large quark-initiated jet fraction underlies  $\gamma$ +jet suppression at large  $p_T$ , while the flat spectra give the dominate contribution to  $\gamma$ +jet suppression at low  $p_T$ . We demonstrate that the color charge effect have greater impacts to the ratio  $R_{AA}^{b\text{-jet}} / R_{AA}^{\text{jet}}$  than parton mass effect, which decrease moderately at  $p_T \sim 300$  GeV/ $c$ . Such a systematic extraction of jet energy loss distributions can help constrain model uncertainties and pave the way to precise predictions of the properties of the hot QCD medium created in relativistic heavy-ion collisions<sup>2</sup>.

Several caveats should be mentioned. First, due to the limited data, we ignore the jet cone dependence [50, 85] at present and mainly focus on a qualitative investigation on the effects from the initial spectrum and parton mass/ flavor on the jet  $R_{AA}$ . For a more strict study, we should use measurements with the same  $R$  in a global analysis. With the upcoming high precision measurements of  $b$ -jet  $R_{AA}$  at the LHC, one can quantitatively analyse those mass/ flavor dependent jet quenching. Second, the MCMC bands is more restricted than the uncertainty in the experimental data. A more detailed treatment in the Bayesian analysis of the uncertainties is needed in the future. Finally, the Bayesian analysis here uses specific functional form for the parameterization, thus introducing long-range correlations in the parameter space which may potentially bias the extracted parameters. A possible solution to tackle such issue is

<sup>2</sup> When finalizing this paper, the authors notice a very recent parallel study of extracting the flavor dependence of parton energy loss [88], but from the nuclear modifications of various hadron species instead of jet observables presented in our work.

to use information field based approach as presented in Ref. [74].

**Acknowledgments:** This research is supported by

National Natural Science Foundation of China with Project Nos. 12035007, 12022512, 12147131, Guangdong Major Project of Basic and Applied Basic Research No. 2020B0301030008. S.Z. is further supported by the MOE Key Laboratory of Quark and Lepton Physics (CCNU) under Project No. QLPL2021P01.

- 
- [1] C. Adler *et al.*, Phys. Rev. Lett. **89**, 202301 (2002).
  - [2] C. Adler *et al.* [STAR], Phys. Rev. Lett. **90** (2003), 082302
  - [3] G. Aad *et al.* [ATLAS Collaboration], Phys. Rev. Lett. **105**, 252303 (2010).
  - [4] S. Chatrchyan *et al.* [CMS Collaboration], Phys. Lett. B **718**, 773 (2013);
  - [5] G. Aad *et al.* [ATLAS Collaboration], Phys. Rev. Lett. **114**, no. 7, 072302 (2015)
  - [6] S. Chatrchyan *et al.* [CMS Collaboration], Phys. Lett. B **730**, 243 (2014)
  - [7] X. N. Wang and M. Gyulassy, Phys. Rev. Lett. **68**, 1480 (1992).
  - [8] X. N. Wang, Phys. Rev. C **61**, 064910 (2000)
  - [9] G. Y. Qin, J. Ruppert, C. Gale, S. Jeon, G. D. Moore and M. G. Mustafa, Phys. Rev. Lett. **100**, 072301 (2008).
  - [10] X. -F. Chen, T. Hirano, E. Wang, X. -N. Wang and H. Zhang, Phys. Rev. C **84**, 034902 (2011).
  - [11] A. Buzzatti and M. Gyulassy, Phys. Rev. Lett. **108**, 022301 (2012).
  - [12] A. Majumder and C. Shen, Phys. Rev. Lett. **109**, 202301 (2012).
  - [13] K. Aamodt *et al.* [ALICE Collaboration], Phys. Lett. B **696**, 30 (2011).
  - [14] S. Chatrchyan *et al.* [CMS Collaboration], Eur. Phys. J. C **72**, 1945 (2012).
  - [15] J. W. Qiu, F. Ringer, N. Sato and P. Zurita, Phys. Rev. Lett. **122**, no.25, 252301 (2019)
  - [16] X. N. Wang, Z. Huang and I. Sarcevic, Phys. Rev. Lett. **77**, 231 (1996)
  - [17] T. Renk, Phys. Rev. C **74**, 034906 (2006).
  - [18] H. Zhang, J. F. Owens, E. Wang and X.-N. Wang, Phys. Rev. Lett. **103**, 032302 (2009).
  - [19] G. Y. Qin, J. Ruppert, C. Gale, S. Jeon and G. D. Moore, Phys. Rev. C **80**, 054909 (2009).
  - [20] A. Adare *et al.* [PHENIX Collaboration], Phys. Rev. C **80**, 024908 (2009).
  - [21] B. I. Abelev *et al.* [STAR Collaboration], Phys. Rev. C **82**, 034909 (2010).
  - [22] W. Chen, S. Cao, T. Luo, L. G. Pang and X. N. Wang, Phys. Lett. B **777**, 86 (2018)
  - [23] W. Dai, I. Vitev and B. -W. Zhang, Phys. Rev. Lett. **110**, 142001 (2013).
  - [24] R. B. Neufeld, I. Vitev and B. W. Zhang, Phys. Rev. C **83**, 034902 (2011)
  - [25] Z. B. Kang, I. Vitev and H. Xing, Phys. Rev. C **96**, no. 1, 014912 (2017)
  - [26] T. Luo, S. Cao, Y. He and X. N. Wang, Phys. Lett. B **782** (2018), 707-716
  - [27] S. L. Zhang, T. Luo, X. N. Wang and B. W. Zhang, Phys. Rev. C **98** (2018), 021901
  - [28] S. L. Zhang, X. N. Wang and B. W. Zhang, Phys. Rev. C **105**, no.5, 5 (2022)
  - [29] A. M. Sirunyan *et al.* [CMS], Phys. Rev. Lett. **119**, no.8, 082301 (2017)
  - [30] Z. Yang, W. Chen, Y. He, W. Ke, L. Pang and X. N. Wang, Phys. Rev. Lett. **127** (2021) no.8, 082301
  - [31] S. L. Zhang, H. Xing and B. W. Zhang, Sci. China Phys. Mech. Astron. **66**, no.12, 121012 (2023)
  - [32] H. Zhang, J. F. Owens, E. Wang and X. N. Wang, Phys. Rev. Lett. **98**, 212301 (2007).
  - [33] C. Adler *et al.*, Phys. Rev. Lett. **90**, 082302 (2003).
  - [34] A. Ayala, J. Jalilian-Marian, J. Magnin, A. Ortiz, G. Paic and M. E. Tejeda-Yeomans, Phys. Rev. Lett. **104**, 042301 (2010)
  - [35] A. Ayala, J. Jalilian-Marian, A. Ortiz, G. Paic, J. Magnin and M. E. Tejeda-Yeomans, Phys. Rev. C **84**, 024915 (2011)
  - [36] S. L. Zhang, M. Q. Yang and B. W. Zhang, Eur. Phys. J. C **82**, no.5, 414 (2022)
  - [37] N. B. Chang, Y. Tachibana and G. Y. Qin, Phys. Lett. B **801** (2020), 135181
  - [38] R. Kunnawalkam Elayavalli and K. C. Zapp, JHEP **07** (2017), 141
  - [39] Z. B. Kang, F. Ringer and W. J. Waalewijn, JHEP **07** (2017), 064
  - [40] G. L. Ma, Phys. Rev. C **89** (2014) no.2, 024902
  - [41] S. Chatrchyan *et al.* [CMS Collaboration], Phys. Rev. C **90**, no. 2, 024908 (2014)
  - [42] M. Aaboud *et al.* [ATLAS], Phys. Rev. Lett. **123**, no.4, 042001 (2019)
  - [43] M. Aaboud *et al.* [ATLAS Collaboration], Eur. Phys. J. C **77** (2017) no.6, 379
  - [44] I. Vitev, S. Wicks and B. W. Zhang, JHEP **11** (2008), 093
  - [45] J. Adams *et al.* [STAR], Phys. Rev. Lett. **92**, 052302 (2004)
  - [46] Y. He, W. Chen, T. Luo, S. Cao, L. G. Pang and X. N. Wang, Phys. Rev. C **106**, no.4, 044904 (2022)
  - [47] A. M. Sirunyan *et al.* [CMS], Phys. Lett. B **776**, 195-216 (2018)
  - [48] M. Aaboud *et al.* [ATLAS], Eur. Phys. J. C **78**, no.12, 997 (2018)
  - [49] G. Y. Qin and X. N. Wang, Int. J. Mod. Phys. E **24**, no.11, 1530014 (2015)
  - [50] A. M. Sirunyan *et al.* [CMS], JHEP **05**, 284 (2021)
  - [51] L. Apolinário, Y. J. Lee and M. Winn, Prog. Part. Nucl. Phys. **127**, 103990 (2022)
  - [52] Yuri L. Dokshitzer and D. E. Kharzeev, Phys. Lett. B, 519:199-206, 2001.
  - [53] B. W. Zhang, E. Wang and X. N. Wang, Phys. Rev. Lett. **93**, 072301 (2004)
  - [54] M. Djordjevic and M. Gyulassy, Phys. Lett. B **560**, 37-43 (2003)
  - [55] N. Armesto, C. A. Salgado and U. A. Wiedemann, Phys. Rev. D **69**, 114003 (2004).
  - [56] P. Gras, S. Höche, D. Kar, A. Larkoski, L. Lönnblad, S. Plätzer, A. Siódmok, P. Skands, G. Soyez and J. Thaler, JHEP **07**, 091 (2017)
  - [57] C. Frye, A. J. Larkoski, J. Thaler and K. Zhou, JHEP

- 09**, 083 (2017)
- [58] Y. T. Chien and R. Kunnawalkam Elayavalli, [arXiv:1803.03589 [hep-ph]].
  - [59] S. Y. Chen, B. W. Zhang and E. K. Wang, Chin. Phys. C **44**, no.2, 024103 (2020)
  - [60] A. M. Sirunyan *et al.* [CMS], JHEP **07**, 115 (2020)
  - [61] H. T. Li and I. Vitev, Phys. Rev. D **101**, 076020 (2020)
  - [62] J. Yan, S. Y. Chen, W. Dai, B. W. Zhangy and E. Wang, Chin. Phys. C **45**, no.2, 024102 (2021)
  - [63] A. M. Sirunyan *et al.* [CMS], Phys. Rev. Lett. **119**, no.8, 082301 (2017)
  - [64] M. Aaboud *et al.* [ATLAS], Phys. Rev. Lett. **123** (2019) no.4, 042001
  - [65] G. Aad *et al.* [ATLAS], Phys. Lett. B **846**, 138154 (2023)
  - [66] G. Aad *et al.* [ATLAS], Eur. Phys. J. C **83** (2023) no.5, 438
  - [67] M. Aaboud *et al.* [ATLAS], Phys. Lett. B **790**, 108-128 (2019)
  - [68] Y. He, S. Cao, W. Chen, T. Luo, L. G. Pang and X. N. Wang, Phys. Rev. C **99**, no.5, 054911 (2019)
  - [69] S. L. Zhang, J. Liao, G. Y. Qin, E. Wang and H. Xing, Sci. Bull. **68**, 2003-2009 (2023)
  - [70] J. Alwall, R. Frederix, S. Frixione, V. Hirschi, F. Maltoni, O. Mattelaer, H. S. Shao, T. Stelzer, P. Torrielli and M. Zaro, JHEP **07**, 079 (2014)
  - [71] Y. He, L. G. Pang and X. N. Wang, Phys. Rev. Lett. **122**, no.25, 252302 (2019)
  - [72] Y. Xu, J. E. Bernhard, S. A. Bass, M. Nahrgang and S. Cao, Phys. Rev. C **97**, no.1, 014907 (2018)
  - [73] S. Cao *et al.* [JETSCAPE], Phys. Rev. C **104**, no.2, 024905 (2021)
  - [74] M. Xie, W. Ke, H. Zhang and X. N. Wang, Phys. Rev. C **108** (2023) no.1, L011901
  - [75] C. Andrieu, N. de Freitas, A. Doucet, M.I. Jordan Mach.Learn. 50 (2003) 5.
  - [76] A. Banfi, G. P. Salam and G. Zanderighi, JHEP **07**, 026 (2007)
  - [77] M. Cacciari, G. P. Salam and G. Soyez, JHEP **04** (2008), 063
  - [78] M. Cacciari, G. P. Salam and G. Soyez, Eur. Phys. J. C **72**, 1896 (2012).
  - [79] W. Dai, M. Z. Li, B. W. Zhang and E. Wang, [arXiv:2205.14668 [hep-ph]].
  - [80] X. N. Wang, Phys. Rev. C **58**, 2321 (1998)
  - [81] W. Liu, C. M. Ko and B. W. Zhang, Phys. Rev. C **75**, 051901 (2007)
  - [82] X. Chen, H. Zhang, B. W. Zhang and E. Wang, J. Phys. **37**, 015004 (2010)
  - [83] W. J. Xing, S. Cao, G. Y. Qin and H. Xing, Phys. Lett. B **805**, 135424 (2020)
  - [84] V. Khachatryan *et al.* [CMS], Phys. Rev. C **96**, no.1, 015202 (2017)
  - [85] G. Aad *et al.* [ATLAS], Phys. Lett. B **719**, 220-241 (2013)
  - [86] J. Huang, Z. B. Kang and I. Vitev, Phys. Lett. B **726**, 251-256 (2013)
  - [87] W. A. Horowitz and M. Gyulassy, Phys. Lett. B **666**, 320-323 (2008)
  - [88] W. J. Xing, S. Cao and G. Y. Qin, Phys. Lett. B **850**, 138523 (2024)